

of the first two bands relative to that of the last band compared with the high relative intensity found for these bands in the melt could be due to a change in the character of the hydrogen bonding, which might affect especially the intensity of bending modes.

It is interesting to note that an equilibrium between HSO_4^- , H_2O , and $\text{S}_2\text{O}_7^{2-}$ (i.e. eq 1) could give rise to temperature-related isosbestic points. However, it should be emphasized that the existence of the temperature-related isosbestic point at $6.4 \times 10^3 \text{ cm}^{-1}$, shown in Figure 4, is not a proof for the involvement of eq 1, especially since internal linearity of the spectra is not found over the entire wavelength range measured.

An extensive computer calculation on the basis of the observed spectra and of the type described earlier^{1,25} of species concentrations and thermodynamic data is not justified due to the large variation in solvent composition, ionic strength, temperature, and vapor pressure.

Conclusion

Both the Raman spectra and the absorption spectra of molten $\text{KHSO}_4\text{-K}_2\text{S}_2\text{O}_7$ mixtures can be interpreted in accordance with eq 1. The dominating species formed in the temperature range investigated are HSO_4^- , H_2O , and $\text{S}_2\text{O}_7^{2-}$. Parameters that influence the relative concentration of these species are the initial compositions of the melts, the temperature, and the vapor pressure of water, which in the present investigation is equal to the equilibrium pressure at the actual temperature. The structure of $\text{S}_2\text{O}_7^{2-}$ in the melt most probably corresponds to the point group C_{2v} . The structure

of HSO_4^- is most likely C_s . Different types of hydrogen bonding probably occur between the three main species in the melt depending on the temperature. Due to the rather low vapor pressures of the melts also at elevated temperatures, the water molecules must be associated strongly to the sulfur-containing species. Such an association possibly involves either three hydrogen bonds or two hydrogen bonds and a third bond (e.g. a electrostatic (dipole-dipole) bonding between a lone pair on the oxygen atom and a pyrosulfate ion).

Unfortunately, due to the many unknown parameters involved, the spectra cannot be used for quantitative estimations of, for example, species concentrations and equilibrium constants. However, the intensity of the Raman bands of HSO_4^- compared with the intensities of $\text{S}_2\text{O}_7^{2-}$ bands at 430°C might be used to estimate the initial composition of any melt composed of KHSO_4 and $\text{K}_2\text{S}_2\text{O}_7$ under the assumption that the melt is examined at the equilibrium pressure.

An extended knowledge of these molten mixtures is useful in the study of redox equilibria, complex formation, and solubility of solute vanadium species, as will be shown in a later paper.²⁶

Acknowledgment. R. W. Berg is thanked for assistance in connection with the measurements of some of the Raman spectra and for useful comments. Further thanks are due to the Danish Technical Science Research Foundation for financial support.

Registry No. $\text{K}_2\text{S}_2\text{O}_7$, 7790-62-7; KHSO_4 , 7646-93-7; $\text{S}_2\text{O}_7^{2-}$, 16057-15-1; HSO_4^- , 14996-02-2.

(25) Fehrmann, R.; Bjerrum, N. J.; Pedersen, E. *Inorg. Chem.* **1982**, *21*, 1497.

(26) Fehrmann, R.; Hansen, N. H.; Bjerrum, N. J.; Philipsen, J.; Pedersen, E., to be submitted for publication.

Contribution from the Department of Chemistry, Princeton University, Princeton, New Jersey 08544

Resonance Raman Enhancement of Imidazole Vibrations via Charge-Transfer Transitions of Pentacyanoiron(III) Imidazole and Imidazolate Complexes

M. ANTON WALTERS and THOMAS G. SPIRO*

Received December 20, 1982

Modest enhancement is observed for Raman modes of the bound imidazole (ImH) in $[(\text{ImH})\text{Fe}(\text{CN})_5]^{2-}$ upon laser excitation in a broad, weak absorption band at $\sim 480 \text{ nm}$, which is assignable, on the basis of excitation profiles, to overlapping charge-transfer transitions from the two highest ImH π orbitals to the Fe^{III} d_x vacancy. Similar enhancement is seen for Im⁻ modes in $[(\text{Im})\text{Fe}(\text{CN})_5]^{3-}$ upon excitation in a weak band at $\sim 650 \text{ nm}$ and a strong band at $\sim 440 \text{ nm}$, which are suggested to be the two π CT transitions, the π orbitals being split by the bonding alterations accompanying deprotonation of the bound ImH. The Fe-imidazole stretching vibration is weak or absent in these spectra, consistent with the nonbonding character of the Fe terminal orbital. Detection of ring modes of ImH or Im⁻ bound to low-spin Fe^{III} in heme proteins may require a concentration of $\sim 25 \text{ mM}$ if similar CT transitions can be located and excited. Detection limits might be lower if the CT dipole strengths are increased in the proteins via favorable orientations of the imidazole rings.

Introduction

Transition-metal ions are commonly bound to proteins via histidine side chains, due to the σ donor strength of the imidazole and the moderate pK_a (~ 7) of the imidazolium ion.¹ Spectroscopic probes of bound imidazole are therefore useful in studying metalloproteins. The vibrational modes of bound imidazole can in principle be monitored by Raman spectroscopy. To attain adequate sensitivity, however, and, more importantly, to discriminate against unbound imidazole, it is necessary to employ resonance enhancement² via selective excitation of electronic transitions involving the bound imid-

azole. Charge-transfer (CT) transitions from imidazole to the metal ion or vice versa are attractive in this regard.

Heme proteins are of particular interest, because at least one of the heme axial ligands is usually imidazole. However, CT transitions are difficult to locate because the absorption spectrum is dominated by the intense porphyrin $\pi\text{-}\pi^*$ transitions. We have observed large enhancements of bound pyridine (py) modes in $(\text{py})_2\text{Fe}^{\text{II}}(\text{MP})$ (MP = mesoporphyrin IX) via a transition at $\sim 490 \text{ nm}$ assigned to $\text{Fe}^{\text{II}}(d_x) \rightarrow \text{py}(\pi^*)$ CT.³ Since the π^* orbitals of imidazole (ImH) are higher in energy than those of Py, analogous $\text{Fe}^{\text{II}}(d_x) \rightarrow$

(1) Sundberg, R. J.; Martin, R. B. *Chem. Rev.* **1974**, *74*, 471.

(2) Spiro, T. G.; Stein, P. *Annu. Rev. Phys. Chem.* **1977**, *28*, 501.

(3) Wright, P. G.; Stein, P.; Burke, J. M.; Spiro, T. G. *J. Am. Chem. Soc.* **1979**, *101*, 3531.

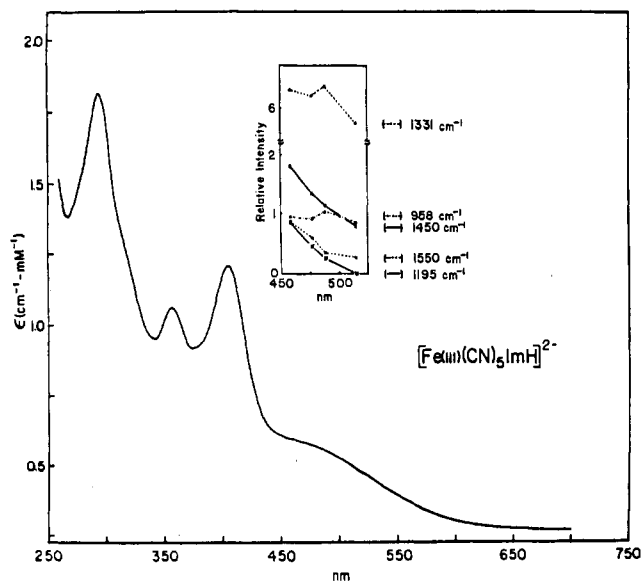


Figure 1. Absorption spectrum for $[(\text{CN})_5\text{Fe}^{\text{III}}\text{ImH}]^{2-}$ in H_2O (pH 7.0) and excitation profiles (inset) for several Raman bands.

$\text{ImH}(\pi^*)$ transitions are expected in the ultraviolet, and may be inaccessible. However $\text{ImH} \rightarrow \text{metal}$ CT transitions lie in the near-UV for tetragonal Cu^{II} ^{4,5} and may be lower in energy for Fe^{III} . Indeed visible absorption bands attributable to such transitions have been reported by Sheperd^{6a} for ImH and Im^- complexes of $[\text{Fe}(\text{CN})_5]^{2-}$. Accordingly we have studied the resonance Raman (RR) spectra of these complexes as possible models for low-spin Fe^{III} heme proteins with ImH or Im^- axial ligands. Enhancement of ring modes is observed, although the enhancement factors are modest, presumably, due to the weakness and breadth of the absorption bands. The enhancement patterns are useful in understanding the character of the CT transitions. Fairly concentrated samples will be required if similar transitions are used to monitor bound imidazole modes in heme proteins.

Experimental Section

$\text{Na}_3[\text{Fe}(\text{CN})_5\text{NH}_3] \cdot 3\text{H}_2\text{O}$ was prepared from $\text{Na}_2[\text{Fe}(\text{CN})_5\text{NO}]$ by the method reported by Lux.⁷ This procedure was modified by the addition of NaOH to catalyze the reaction and the use of ethanol to precipitate the product.⁸ The dried product was dissolved in $\sim 6\%$ H_2O_2 containing at least a 5-fold excess of imidazole. The reaction mixture was then placed in an ice bath and kept in darkness for approximately 45 min to allow the formation of $\text{Fe}^{\text{III}}(\text{CN})_5(\text{imidazole})$. A few milligrams of Pt/activated charcoal was then added to the chilled solution to decompose the excess H_2O_2 . The charcoal was removed by filtration, and the solution pH was adjusted with H_2SO_4 or NaOH for the formation of either $[(\text{ImH})\text{Fe}(\text{CN})_5]^{2-}$ or $[(\text{Im})\text{Fe}(\text{CN})_5]^{2-}$.

Resonance Raman spectra were obtained via backscattering from a spinning cell with Kr^+ laser excitation. The scattered light was detected with a Spex 1401 double monochromator and cooled photomultiplier. Data were collected and stored in a Digital Equipment Corporation MINC 11 computer.

Results and Discussion

Figure 1 shows the absorption spectrum of $[(\text{ImH})\text{Fe}(\text{CN})_5]^{2-}$ (I). The three near-UV bands of I are very similar to those observed for $[(\text{NH}_3)\text{Fe}(\text{CN})_5]^{2-}$ by Gale and

McCaffery.⁹ They assigned the first and third of these to $\text{CN}^-(\pi) \rightarrow \text{Fe}^{\text{III}}(d_\pi)$ transitions, based on their similarity in absorption and MCD spectra, to those displayed by $\text{Fe}(\text{CN})_6^{3-}$. The middle band, at 370 nm, was assigned to a CT transition from the NH_3 lone pair (n) orbital.⁹ A similar assignment, $\text{ImH}(n) \rightarrow \text{Fe}^{\text{III}}(d_\pi)$ CT, is plausible for the 360-nm band of I. The ionization potential for the n orbital is 0.5 eV lower for ImH than for NH_3 , but the bonding interaction with a $\text{Fe}^{\text{III}}d_\pi$ orbital may diminish the difference, and the observed 750- cm^{-1} upshift of the ImH CT band seems reasonable.

Schugar and co-workers have recently analyzed $\text{ImH} \rightarrow \text{Cu}^{\text{II}}(d_{x^2-y^2})$ CT absorptions, using solid-state complexes of known structure.^{4,5} They assigned transitions from the three highest ImH orbitals, π_1 , π_2 , and n , in order of decreasing energy. The σ CT transition, $n \rightarrow \text{Cu}^{\text{II}}$, was always found as an intense band at ~ 220 nm, whereas the two π CT transitions, $\pi_2 \rightarrow \text{Cu}^{\text{II}}$, and $\pi_1 \rightarrow \text{Cu}^{\text{II}}$, were found as weaker bands at longer wavelengths, ~ 250 and ~ 320 nm, but with energies and intensities that varied for different dihedral angles between the imidazole and Cu^{II} -ligand planes, reflecting differing π_1 - or π_2 - $d_{x^2-y^2}$ overlaps. In aqueous solution $(\text{ImH})_4\text{Cu}^{2+}$ shows weak ($\epsilon \sim 300 \text{ M}^{-1}$) and broad absorption over the 260–340-nm range, which was attributed to multiple overlapping π CT transitions due to free rotation of the ImH ligands about their bonds to Cu^{II} in solution.⁴

CT transitions to low-spin Fe^{III} are expected at lower energy than those to Cu^{II} , since there is a vacancy in the d_π orbital set. The above assignments place the energy difference for the $\text{ImH}(n)$ CT transition at $\sim 18\,000 \text{ cm}^{-1}$. We therefore expect, by analogy with $(\text{ImH})_4\text{Cu}^{2+}$, a broad absorption in the vicinity of 500 nm due to overlapping $\text{ImH}(\pi)$ CT transitions in I. This is indeed observed (Figure 1), and Sheperd⁶ assigned this absorption to $\text{ImH} \rightarrow \text{Fe}^{\text{III}}$ CT on the basis of its variability for substituted imidazoles and of a linear correlation of its energy with the long-wavelength band for $[(\text{N}-\text{H}_3)_2\text{Ru}^{\text{III}}]$ complexes¹⁰ of the same imidazoles.

The $\text{ImH}(\pi) \rightarrow \text{Fe}^{\text{III}}$ CT character of the broad ~ 480 -nm band is supported by the resonance Raman (RR) spectrum (Figure 2), which shows a number of enhanced ImH ring modes. The intensity pattern is quite different from that of the free ImH nonresonant Raman spectrum (Figure 3); for example, the 1261- cm^{-1} band is the strongest one for ImH , while the RR spectrum of I shows only a weak band at 1269 cm^{-1} , but a very strong band at 1331 cm^{-1} . Such relative intensity changes are attributable to excited-state distortions associated with transitions from specific π orbitals. Moreover the assignment of the broad ~ 480 -nm absorption band to overlapping contributions from different $\text{ImH}(\pi)$ CT transitions is supported by excitation profiles (Figure 1 inset) which show that some of the RR bands (1550, 1450, 1195 cm^{-1}) lose intensity much faster than others (1331, 958 cm^{-1}) as the laser is tuned to longer wavelengths within the absorption envelope. The latter bands peak somewhat to the blue side of 4579 Å; excitation at 4067 Å, in resonance with the 405-nm $\text{CN}(\pi) \rightarrow \text{Fe}^{\text{II}}(d_\pi)$ transition, gave no detectable enhancement of ImH modes.

Excitation at 3638 Å, within the $\text{ImH}(n)$ CT band, likewise failed to produce detectable enhancement. From the intensity of 983- cm^{-1} band of SO_4^{2-} , present as an internal standard, we estimate that we would easily have seen ImH mode spectra if their enhancements were as much as one-half those observed at 4579 Å. The lower enhancement is attributable to smaller Franck-Condon factors for the ImH ring modes. Perturbation of the ring should be smaller for the n than the π CT transition,

- (4) Bernarducci, E. F.; Schwindinger, W. F.; Hughey, J. L.; Krogh-Jespersen, K.; Schugar, H. J. *J. Am. Chem. Soc.* **1981**, *103*, 1686.
- (5) Faucett, T. G.; Bernarducci, E. E.; Krogh-Jespersen, K.; Schugar, H. J.; *J. Am. Chem. Soc.* **1980**, *102*, 2598.
- (6) (a) Sheperd, R. E. *J. Am. Chem. Soc.* **1976**, *98*, 3329. (b) Johnson, C. R.; Sheperd, R. E.; Marr, B.; O'Donnel, S.; Dressick, W. *J. Am. Chem. Soc.* **1980**, *102*, 6227.
- (7) Lux, H. In "Handbook of Preparative Inorganic Chemistry"; Brauer, G., Ed.; Academic Press, 1965; Vol. II, p 1512.
- (8) Sheperd, R. E. personal communication.

- (9) Gale, R.; McCaffery, A. J. *J. Chem. Soc., Dalton Trans.* **1973**, 1344.
- (10) (a) Sundberg, R. G.; Bryan, R. F.; Taylor, I. V.; Taube, H. *J. Am. Chem. Soc.* **1974**, *96*, 381. (b) Sundberg, R. J.; Gupta, G. *Bioinorg. Chem.* **1973**, *3*, 39.

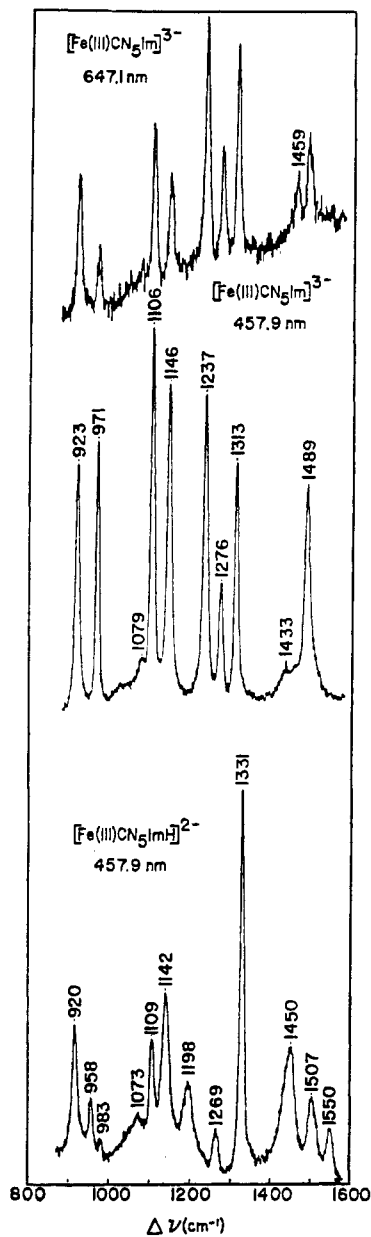


Figure 2. RR spectra for $[(\text{CN})_5\text{Fe}^{\text{III}}\text{Im}]^{3-}$ (2×10^{-3} M, pH 12) at 6471 and 4579 Å (peak frequencies are the same except for the extra band at 1459 cm^{-1} excited at 6471 Å) and for $[(\text{CN})_5\text{Fe}^{\text{III}}\text{ImH}]^{2-}$ (2×10^{-3} M, pH 7.0) at 4579 Å. Conditions: 100-mW (4579 Å) or 200-mW (6471 Å) laser power; spectral slit width, 10 cm^{-1} ; scanning at $1 \text{ cm}^{-1}/\text{increment}$, $5 \text{ s}/\text{increment}$.

since the n orbital is nonbonding with respect to the ring.

The absorption spectrum of $[(\text{Im})\text{Fe}(\text{CN})_5]^{3-}$ (II) (Figure 4), shows a strong band at 440 nm, a weak broad band at $\sim 650 \text{ nm}$, and a band at 370 nm of moderate intensity, similar to the 370-nm band of I. Similar transitions are expected for II as for I, with the Im^- CT transitions being influenced by the deprotonation. In general, deprotonation is expected to raise the ImH orbital energies and thus lower the CT transition energies. These effects may be offset by an increase in the strength of the imidazole-iron bond. The two $\text{CN}^- (\pi) \rightarrow \text{Fe}^{\text{III}} (d_{\pi})$ transitions of I, at 300 and 400 nm, are expected at nearly the same energies in II. These positions are overlapped by the $\sim 300\text{-nm}$ end absorption and the strong 440-nm band, respectively.

The 370-nm band is assigned to the imidazole n CT transition, as it is in I. We considered the possibility that the 370-nm band is actually due to contamination by I, but this is ruled out by the EPR spectra (unpublished results), which

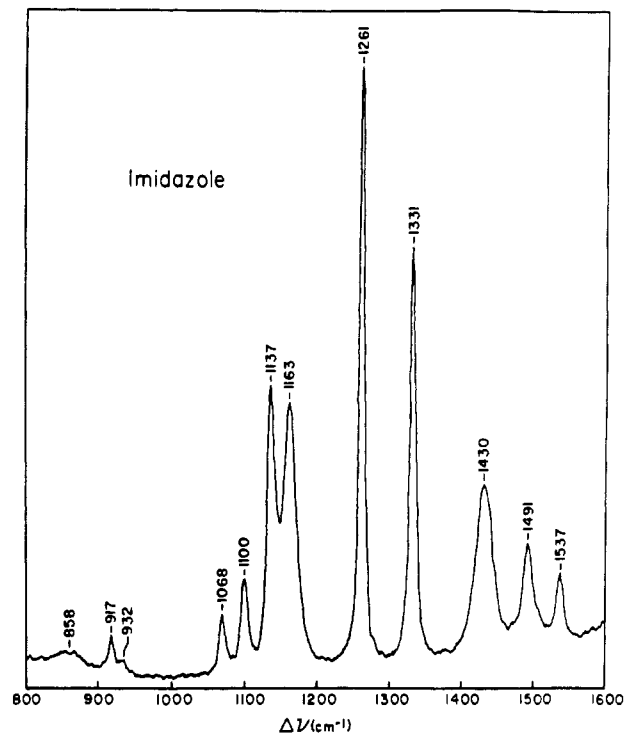


Figure 3. Raman spectrum of 1 M imidazole in H_2O excited at 4880 Å.

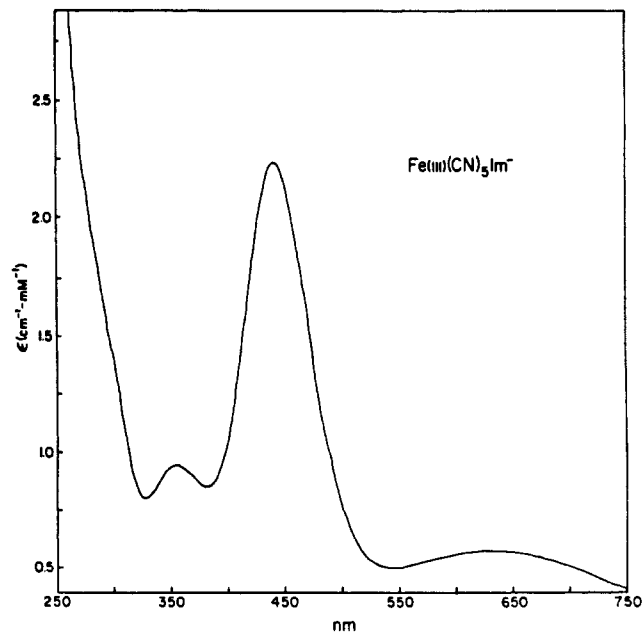


Figure 4. Absorption spectrum for $[(\text{CN})_5\text{Fe}^{\text{III}}\text{Im}]^{3-}$ in H_2O (pH 12).

are quite distinctive for the two species. Nor can it be due to $[\text{Fe}(\text{CN})_5(\text{OH})]^{3-}$ impurity, which has its absorption band at 390 nm and very little absorption at 370 nm.^{6b} The effect of the ImH proton on the energy of the remote n orbital is expected to be slight, and could well be compensated by a stronger $\text{Im}^- - \text{Fe}^{\text{III}}$ σ bond in II. (We note that Schugar and co-workers⁵ report a lowering of the n CT energy of Im^- relative to ImH in Cu^{II} complexes, but the Im^- complex was binuclear, with a Im^- bridge. The interaction of the two equivalent n orbitals might have been responsible for the lowered CT energy).

The two $\text{Im}^- \pi$ CT transitions are then assigned to the strong band at 440 nm and the weak one at 650 nm. The former is at slightly higher energy than the π CT band of I ($\sim 480 \text{ nm}$), while the latter is much ($\sim 5000 \text{ cm}^{-1}$) lower. The large

Table I. Raman Frequencies (cm⁻¹) of Free and Bound ImH and Im⁻

ImH	[(ImH)Fe ^{III} (CN) ₅] ²⁻	[(Im) ⁻ Fe ^{III} (CN) ₅] ³⁻	Im ⁻ ^a
858 (br)			
917	920	923	945
932 (sh)	958	971	
	983		
1068	1073	1079	1075
1100	1109	1106	1100
1137	1142	1146	1143
1163	1198	1237	1249
1261	1269	1276	
1331	1331	1313	1307
1430	1450	1459	1457
1491	1507	1489	
1537	1530		

^a Alkaline solution (3 M KOH) of imidazole (from ref 12).

splitting of the π_1 and π_2 orbitals in II that is implied by this assignment can be rationalized on the basis of differential effects due to deprotonation. One of these orbitals (π_2) is mainly concentrated on the N atom of the ring, while the other (π_1) is mainly concentrated on the C atoms.^{4,5} It is π_2 that is primarily involved in π donation to Fe^{III}; the overlap is expected to increase upon deprotonation, leading to an increase in the transition energy and also in the absorption strength. The strong 440-nm band is assigned to Im⁻(π_2) \rightarrow Fe(d_{xy}). In contrast, the π_1 orbital does not interact with the Fe^{III}, and its energy is raised upon ImH deprotonation, lowering the transition energy. The weak 650-nm band is assigned to Im⁻(π_1) \rightarrow Fe(d_{xz}).

Excitation in either the 440-nm band (4579 Å) or the 650-nm band (6471 Å) produces resonance enhancement of Im⁻ ring modes comparable in extent to those observed for I in its π CT band (Figure 2). The similar intensities for the π_1 and π_2 CT bands of II, despite the greater absorption strength for the latter, are consistent with π_2 being more strongly involved in Im-Fe bonding and less strongly involved in intra-ring bonding than π_1 .

Alteration in the ground-state structure of ImH upon binding to the Fe(CN)₅²⁻ unit is small, as shown by the ring mode frequencies (Table I); most of them are slightly higher in I than in free ImH. Similar small shifts were observed on complexation of ImH with Co^{II}.^{11,12} Other small frequency shifts are observed upon deprotonation of the bound ImH. The frequencies for II are similar to the imidazolate frequencies reported by Yoshida et al.¹²

The low-frequency region of the spectrum was examined for evidence of the Fe-ImH stretching modes. Only weak bands were observable. For I, they occur at 400 (broad), 270, and 240 cm⁻¹. The first of these is assignable to Fe-C-N bending.¹³ One of the remaining pair may be due to $\nu_{\text{Fe-ImH}}$,

the other arising, perhaps, from C-Fe-C bending. The evident weakness of the Fe-ImH mode is attributable to both orbitals in the CT transition, ImH(π) and Fe(d_{xz}) being weakly bonding with respect to the Fe-ImH bond. The low-frequency region for II was obscured by a high background, possibly arising from fluorescent impurities.

The absolute Raman intensities in these resonance-enhanced spectra are modest. The molar intensity of the strongest peak of I, at 1331 cm⁻¹, is 4.1 times greater than that of the 981-cm⁻¹ (ν_1) SO₄²⁻ band when measured at 4579 Å. (The absorption correction is negligible since the absorbance varies slowly in this region; see Figure 1.) This relatively low enhancement is attributable to the low absorptivity and large width of the CT transitions.² Similarly low enhancements can be expected for solution complexes of Cu²⁺ with ImH, in view of the similarly weak and broad CT bands observed.⁴ In this case, however, the Cu-ImH stretching modes may be more prominent, since the CT acceptor orbital ($d_{x^2-y^2}$) is σ , and the Cu-ImH bonds should be weakened in the CT excited state.

Observation of resonance-enhanced bands of coordinated ImH in Fe and Cu proteins will not be easy, if similar enhancements apply. Since the ν_1 SO₄²⁻ band is conveniently monitored down to a level of ~ 0.1 M, the required protein concentration may be 25 mM or higher. Moreover, uncoordinated histidine side chains might interfere if present in large numbers. With 4579-Å excitation, the molar intensity of the 1331-cm⁻¹ band is 15.4 times greater for I than for imidazole itself. It is possible, however, that enhancements will be greater in the proteins, since the orientation of the imidazole ring with respect to the metal ion is held fixed by the polypeptide chain. As shown by Schugar and co-workers,^{4,5} this can lead to intensification and sharpening of the CT bands.

Another uncertainty for protein studies is locating the position of the CT bands, since they can readily be obscured by stronger absorptions. In heme proteins, the intense π - π^* porphyrin transitions dominate the entire visible region. Low-spin Fe^{III} hemes with one or two axial imidazole ligands should have CT transitions similar to those of I, with energy shifts associated with the altered energy of the d_{xz} acceptor orbital. The influence of the porphyrin macrocycle on this orbital should not be very different from that of bound cyanides. Thus the 450-500-nm region, which is in the trough between the B and Q₁ bands of heme proteins, may be a reasonable place to look for coordinated imidazole RR modes. In low-spin Fe^{II} hemes, the d_{xz} orbitals are filled, and the ImH \rightarrow Fe^{II} CT transitions, which must terminate on d_{xz} orbitals, are expected in the UV region. For high-spin Fe^{III} or Fe^{II} there are many possibilities for terminal d orbitals, whose energies, relative to ImH, are difficult to predict.

Acknowledgment. We thank Dr. S. Groh and Dr. N. Kojima for assistance in acquiring EPR spectra, M. Mitchell for assistance with the Raman spectra, and Dr. B. Holmquist for helpful discussions. This work was supported by NIH Grant HL 12526 and NSF Grant CHE 81-06084.

Registry No. [(CN)₅Fe^{III}ImH]²⁻, 61332-60-3; [(CN)₅Fe^{III}Im]³⁻, 74353-96-1; ImH, 288-32-4.

(11) Salama, S.; Spiro, T. G. *J. Am. Chem. Soc.* **1978**, *100*, 1105.

(12) Yoshida, C. M.; Freedman, T. B.; Loehr, T. M. *J. Am. Chem. Soc.* **1975**, *97*, 1028.

(13) Nakagawa, I.; Shimanouchi, T. *Spectrochim. Acta, Part A* **1970**, *26A*, 131.